Journal of Hydrology 564 (2018) 442–451

Contents lists available at ScienceDirect

Journal of Hydrology

journal homepage: www.elsevier.com/locate/jhydrol

Research papers

Estimating river accommodation capacity for organic pollutants in data-scarce areas

C.S. Zhao[a], S.T. Yang[a], Y. Sun[b], H.T. Zhang[c], C.L. Sun[d], T.R. Xu[e,*], R.P. Lim[f], S.M. Mitrovic[g]

[a] College of Water Sciences, Beijing Key Laboratory of Urban Hydrological Cycle and Sponge City Technology, Beijing Normal University, Beijing 100875, PR China
[b] Jinan Survey Bureau of Hydrology and Water Resources, Jinan 250013, PR China
[c] Dongying Bureau of Hydrology and Water Resources, Dongying 257000, PR China
[d] Beijing Water Authority, Beijing 100038, PR China
[e] State Key Laboratory of Earth Surface Processes and Resource Ecology, Faculty of Geographical Science, Beijing Normal University, Beijing 100875, PR China
[f] School of Life Sciences, Faculty of Science, University of Technology, Sydney, NSW 2007, Australia
[g] Applied Ecology Team, School of Life Sciences, Faculty of Science, University of Technology, Sydney, NSW 2007, Australia

ARTICLE INFO

This manuscript was handled by G. Syme, Editor-in-Chief

Keywords:
Hydrology
Water quality
River
Water environmental capacity
Data-scarce area

ABSTRACT

Globally, water quality degradation severely threatens the security of water resources. Understanding a river's capacity to accommodate pollutants (or water environmental capacity: WEC) can help efficiently protect rivers. However, the requirement for comprehensive ground-observed hydrological and water quality data in previous methods makes it difficult to estimate WEC in areas with limited ground observations. This paper proposes a new framework for WEC estimation in data-scarce areas based on remotely sensed skin water temperature and limited ground observations. Two new models were developed to calculate the two critical parameters for WEC estimation: water temperature, and integrated pollutant degradation coefficients (k). Images of ASTER Surface Kinetic Temperature (AST_08) 90 m grid product were used to retrieve water temperatures. The above results were subsequently used to calculate a river's capacity to accommodate pollutants, or WEC, in agriculturally dominated areas. The use of remote sensing techniques enables the methods to be applied over large spatial scales and to areas with limited ground observations. The application and testing of the framework in four rivers, including two Chinese rivers (the Huai and the Wei Rivers) and two Australian rivers (the Ovens and the Gwydir Rivers), suggest that the models performed well to calculate the real-time water temperature and the coefficient k based on limited ground-observations. Uncertainty analysis on water temperature calculated from remotely sensed land surface temperature and ground-observed meteorological air temperature suggests that remotely sensed water temperature had high concurrence with ground observations (RMSE = 3.08 °C with R^2 = 0.88), while the sparse-spatially distributed meteorological stations reduced the accuracy in estimating water temperature (RMSE = 4.39 °C with R^2 = 0.91). We found that the coefficient (k) increased with water temperature over different seasons in an exponential form but in a logarithmical form with streamflow velocity. Comparison with previous research and other models with abundant data revealed the practicability and effectiveness of our models, which can be easily applied to rivers with insufficient ground observations across the globe.

1. Introduction

Rapid socio-economic development in developing countries has resulted in many quality problems in rivers (Levashova et al., 2004; Liu et al., 2011). Pollution discharged from upstream watersheds and excessive upstream water abstraction has dramatically changed the hydrological regimes and reduce the dilution capacity of a river and may significantly degrade water quality at downstream reaches (Yoon et al., 2015). This deterioration of water quality negatively affects socio-economic development and damages the water ecosystem (Joniak and Kuczyńska-Kippen, 2010; Rui et al. 2015).

The rapid deterioration of river water quality urgently requires effective water quality management strategies to reduce the resulting environmental pressures (Li and Zou, 2015). The most common approach for water quality protection is the use of water quality standards, allowing for the selection of protection levels (Han et al., 2010; Li et al., 2010). Water quality standards, or boundary values for water quality indicators, are then used to calculate the water environmental

* Corresponding author.
E-mail address: xutr@bnu.edu.cn (T.R. Xu).

https://doi.org/10.1016/j.jhydrol.2018.07.022
Received 23 May 2018; Received in revised form 10 July 2018; Accepted 11 July 2018
Available online 18 July 2018

capacity (WEC), or the capacity of a water body to accommodate a certain amount of pollutants, and subsequently to reduce the amount of pollutants discharging into rivers. The WEC has a similar role in water quality protection with the terms "Assimilative Capacity" (Payandeh et al., 2015), "Total Maximum Daily Loads" (Bachmann et al., 2003; Cooter et al., 2010; Kim et al., 2014), etc. (Wang et al., 2015).

Management of the WEC is a key factor to control pollution in rivers (Keller and Cavallaro, 2008). Based on the estimation of the WEC, the total allowable amount of pollutants discharged into rivers can be obtained and allocated appropriately among different industries and areas to ensure that the emission quantities are within the WEC (Chen et al., 2014). A number of methods has emerged for determining the WEC with either simple or complicated mathematical/statistical models (Antonellini et al, 2014; Cuadra and Björklund, 2007; Gong and Jin, 2009; Liu and Borthwick, 2011; Pandey et al, 2011; Zhang et al, 2014b; Wang et al, 2014; Yang et al., 2015). Water quality models with one, two and three dimensions have been used widely and significant progress has been achieved (Imteaz and Asaeda, 2000; Wan et al., 2001; Park et al., 2005; Testa et al., 2013; Li et al., 2015). In general, the models have a high demand for ground observations of hydrology and water quality, as well as for scientific expertise. Several models require extensive field measurement campaigns and also may rely on expert panels, which can lack transparency in making recommendations or are influenced by expert bias (Hughes et al., 2014) that can be very costly (Alcazar et al., 2008). In addition, in many real-world situations, neither the financial capacity nor the necessary scientific expertise is available. Consequently, a lack of effective hydrological and water quality monitoring creates difficulties in river water quality protection (Yu et al., 2015). This significantly restricts the wide application of traditional WEC models in situations with insufficient ground monitoring of hydrological and water quality parameters. Therefore, significantly limited data availability appeals less data-intensive or parsimonious methods, which can be applied in many different situations with limited ground observations (Hughes et al., 2014).

In the WEC models, the rate of pollutant degradation in rivers can be determined by using the integrated degradation coefficient (CAEP, 2003; Dang et al., 2009). The most critical factors influencing the integrated degradation coefficient are water temperature and river discharge (Chen et al., 2007; Gomes and Wai, 2014). For organic pollutants, water temperature is the principal factor influencing the integrated degradation coefficient (Wright and Mcdonell, 1979; Brown and Barnwell, 1987; Li and Liao, 2002; Yang et al., 2014). Therefore, the integrated degradation coefficient for organic pollutants in rivers can be estimated via the water-temperature-dependent function. This greatly facilitates estimation of the WEC in areas with insufficient ground observations for water quality due to the easy access to water temperature estimated via meteorological air-temperature or remotely sensed land surface temperature. This significantly extends the potential to rapidly estimate the WEC in data limited areas. Remote sensing techniques are very convenient in obtaining geo-information from the earth's surface at multiple temporal-spatial scales (Gassman et al., 2007; Nesme et al., 2012), e.g., land-use and vegetation (Leuning et al., 2008; Li et al., 2009; Nesme et al., 2012; Duan et al., 2014), land surface temperature and evapotranspiration (Zhang et al., 2010; Tang et al, 2010, 2011; Duan et al., 2012, 2014), soil moisture (McVicar et al, 2002), catchment drought and runoff (McVicar et al, 2001; Li et al., 2009; Zhang et al., 2009). Moreover, the great advantage for remote sensing in extrapolating land (LST) temperature makes it easy to estimate the WEC in data limited areas. Among all remotely sensed LST, the ASTER Surface Kinetic Temperature (AST_08) product, generated using the five Thermal Infrared (TIR) bands (acquired either during the day or night time), contains LST at 90 m spatial resolution for the land areas and is widely used for studies of volcanism, thermal inertia, surface energy, and high-resolution mapping of fires (refer to https://lpdaac.usgs.gov).

Water surface temperature (WST), including skin (or radiant) WST and bulk WST (Li et al., 2013; Teggi et al., 2014; Zhang et al, 2014a; Wan et al., 2017), is often derived from the methods for land surface temperature (LST). LST and WST are the most commonly remotely-sensed data available for restoration of freshwater ecosystems because water temperature controls the biogeochemical and hydrological processes and plays crucial roles in energy and heat exchanges between water and atmosphere (Alcântara et al., 2010; Thiemann and Schiller, 2003). But the skin WST (e.g., within the upper 0.1 mm of the water surface) can merely reflect the thermal radiation status within a very thin depth under the water surface. Thus it cannot be directly used to replace the bulk WST (e.g., within 10 cm or 4 m below the water surface) (Torgersen et al., 2001) – a key parameter for WEC estimation. In the river ecosystem the photosynthetic rate of phytoplankton, controlling the degeneration rate of organic pollutants and influencing the magnitude of WEC, often occurs in the upper 4 m water layer, e.g., for Lake Constance around noon (Thiemann and Schiller, 2003). A conversion between skin and bulk WSTs has to be made to avoid unexpected uncertainties in the applications (Li et al., 2013). A regional algorithm for bulk temperature was presented for Lake Constance but had high data requirement, e.g., data of air temperature from a weather station within the last three days, which are often hard to get in data-limited regions, restricted its application in other regions across the world (Thiemann and Schiller, 2003). Therefore, it is urgently necessary to develop a new algorithm to convert the remotely-sensed skin WST to bulk WST, or water temperature used for WEC calculation in ground data-limited regions.

Our primary goal was to set up a WEC framework for rivers with limited ground observations, based on the advantages of remote sensing techniques in obtaining data of water surface temperature. Our specific objectives were:

1. To retrieve water temperature by converting remotely sensed skin WST to bulk WST in rivers with limited ground observations;
2. To calculate the integrated degradation coefficient (k) for organic pollutants at any level of temperature; and
3. To estimate the corresponding WEC based on the coefficient (k) for ground-observation limited areas.

This paper is structured around the three objectives in Methods (Section 3), Results and Discussion (Section 4), and Conclusion (Section 5). The data sets used are described in Section 2.

2. Study area and materials

2.1. Study area

The Wei River basin, situated between 103.5 and 110.5°E and 33.5–37.5°N, is located in a continental monsoon climatic zone; the mean temperature ranges from 6 to 14 °C with a mean rainfall of 450–700 mm, and the mean pan evaporation ranges from 1000 to 2000 mm (Li et al., 2014). In recent decades, the entire basin has encountered many serious droughts with long durations and high severity (Huang et al., 2014). The basin is the primary region for agriculture, industry and commerce in Northwestern China (Song et al., 2007). Intensive human activities have resulted in substantial negative impacts on the Wei River, which are characterized by decreasing annual runoff and heavy pollution (Zuo et al., 2014). As a result, 69.2% of the water quality observations exceeded the national water protection standards (e.g., in 2009) and resulted in serious degradation of ecosystem function (Wu et al., 2014b). The two principal issues in terms of pollution in this region are chemical oxygen demand (COD) and ammonia nitrogen (NH_3-N) levels (Zhang et al., 2012), which deserve special attention in future water-resource protection strategies.

Linjiacun (LJC) and Xianyang (XY) are two important hydrological and water quality monitoring stations along the river. The water surface width of this reach ranges from 27 to 500 m and the water depth varies

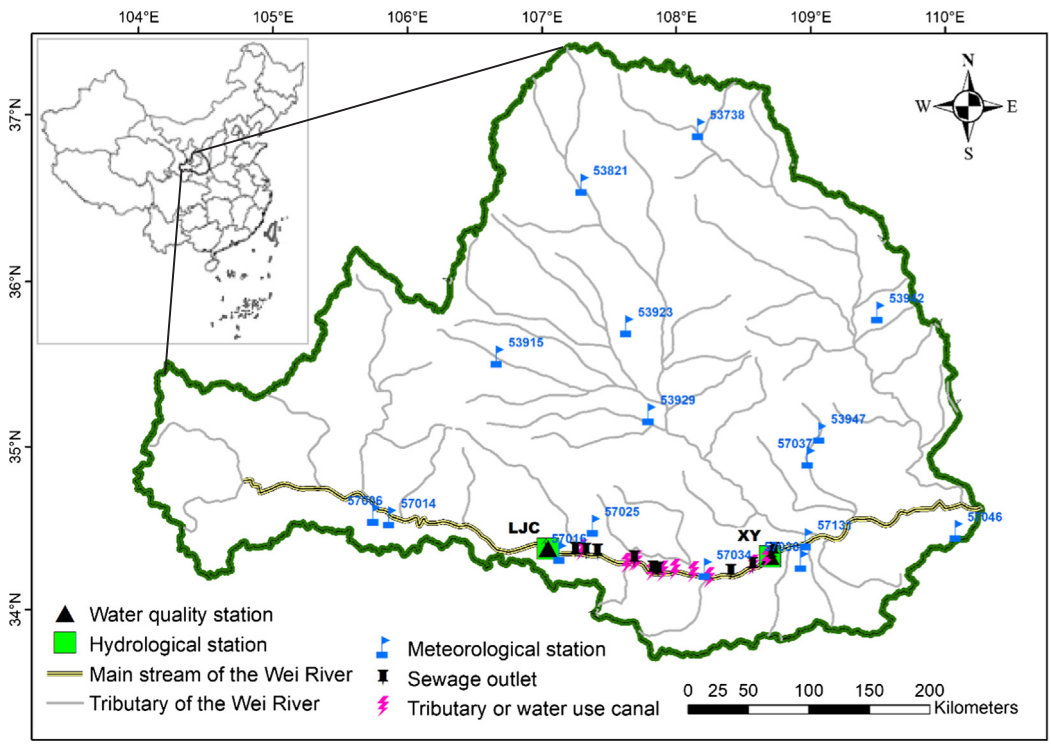

Fig. 1. The Wei River basin and its stations (Partly revised from Zhao et al. (2018)). LJC and XY are two hydrological and water quality monitoring stations on the mainstream of the Wei River with observations collected to test the methodologies in this study.

from 0.25 to 3.9 m varying with reach and season (Feng et al., 2004; Wu et al., 2014a). In the catchment of the river-section between LJC and XY (Fig. 1), many important cities and a large agriculture area are located. Water loss through agricultural activities, industrial wastewater discharge and domestic sewage (Guo et al., 2013) have seriously impacted the health of riverine ecosystems and has significantly restricted the sustainable development of the region. To sustain the local socio-economic development, it is imperative to protect and restore the degraded water quality.

2.2. Dataset

The mainstream of the Wei River between the two water-quality monitoring stations (LJC and XY) was selected to study its WEC. There are 9 sewage outlets, 9 tributaries and 2 water abstraction canals along the 196.91-km length of this river section (Fig. 1). The remotely sensed land surface temperatures (T_s) ASTER Surface Kinetic Temperature (AST_08) 90 m grid product from Jan. 2007 through Dec. 2009 were downloaded from the website (https://lpdaac.usgs.gov). Daily products with cloud cover were excluded to ensure the accuracy of monthly averaged values. T_s for water surface (or WST) within a mixing pixel was calculated using the ESVEP model in Tang and Li (2017) which can separate the net radiation from each other in a riparian mixing pixel as it considers the transmission of direct and diffuse shortwave radiation separately from the transmission of longwave radiation through the canopy. Taking the separated net radiation as a basis, the temperature and evapotranspiration of components in the mixing pixel can be separated. Daily T_s values at the pixel encompassing the water quality stations were selected and averaged as monthly values and subsequently used to construct a water temperature model. All monthly T_s values along the river section from LJC-XY were subsequently inputted into the model to generate the monthly water temperature (T_w) sequences along this river section. Additionally, ground-based air temperature (T_a) data from nearby meteorological stations (Fig. 1) were downloaded from the website of the China Meteorological Administration (CMA) to test the effectiveness of remotely sensed land surface temperature (T_s). In addition, limited ground-based T_w measurements from Jan. 2007 to Dec. 2009 at station LJC were collected. Water quality indicators (COD and NH_3-N) and stream flows at the water-quality monitoring stations LJC and XY, as well as at sewage outlets, water-use canal and tributaries, were measured from Jan. 2007 to Dec. 2009 by the Yellow River Conservancy Commission of the Ministry of Water Resources (MWR), China. All relevant data were subjected to quality control using the quality-control methods of Smirnov et al. (2000) with which the high-frequency temporal instability in the data series was eliminated by application of the criteria of triplet stability.

The water quality standard (C_s, in mg l^{-1}) highly affects the WEC in sections with different water usage. The WEC was determined based on land use and vegetation cover maps drawn from satellite images, as well as industrial statistics data. The water usage of the river section between LJC and XY (Fig. 1) represents the supply of water for both industrial and agricultural activities. Therefore, the C_s for the river section is restricted to 30 mg l^{-1} for COD and 1.5 mg l^{-1} for NH_3-N, according to the national environmental quality criteria for surface water "GB 3838-2002" (EPAC, 2002). Water with concentrations of COD and NH_3-N lower than the corresponding standard values is fit for industrial and agricultural use.

3. Methods

An empirical model for retrieval of water temperatures based on remotely sensed skin water surface temperature is initially presented for rivers with limited ground observations. With this model, the integrated degradation coefficient (k) for organic pollutants at any level of temperature is then calculated. Based on the calculated k, the real-time water environment capacity (WEC) for rivers with limited ground observations can be estimated.

3.1. Retrieval of water temperature

The abundantly available satellite products of skin WST (T_s, in K) bridge the gap to retrieve water temperatures in areas lacking ground

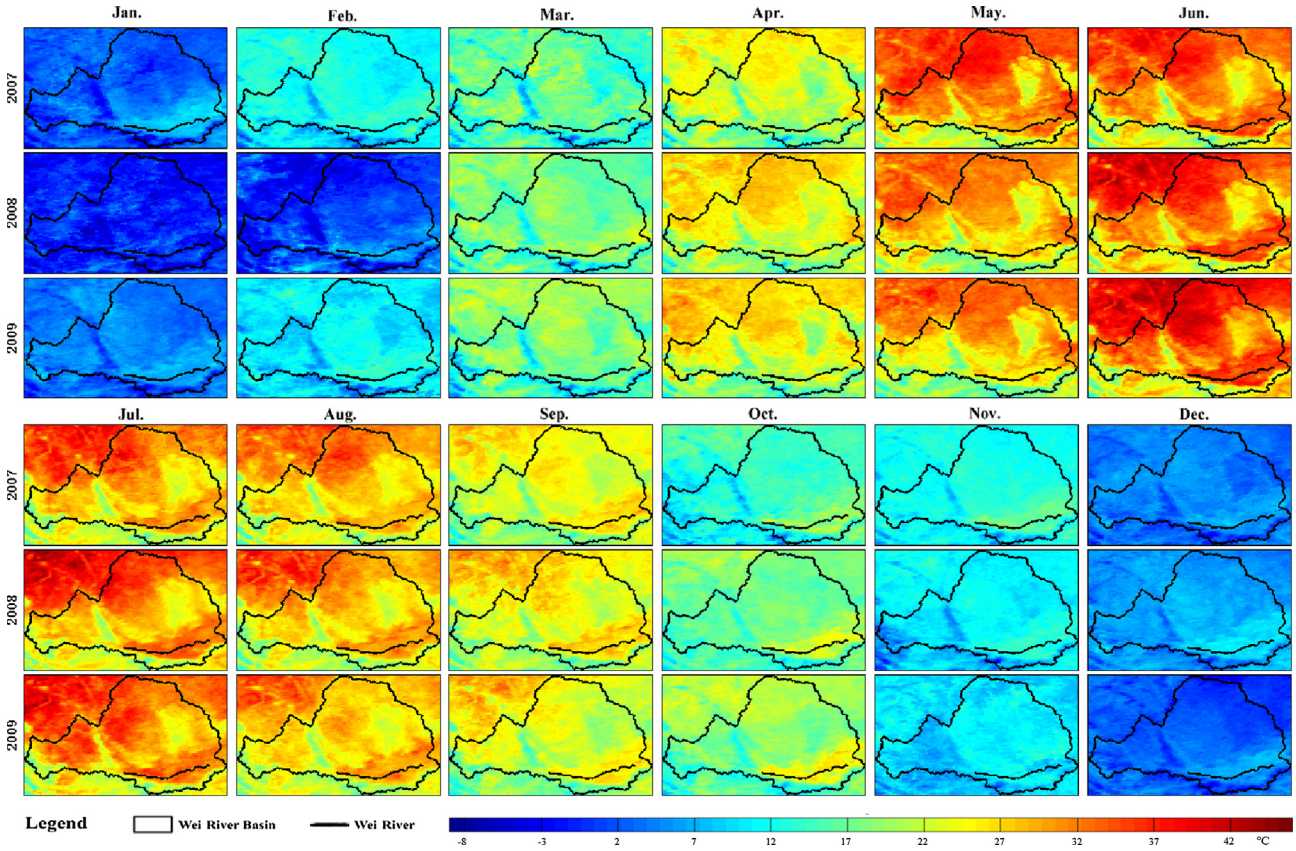

Fig. 2. The monthly ASTER surface-temperature T_s in the Wei River Basin, in K.

observations. In these areas, the monthly bulk WST (T_w, in °C) can be derived from remote-sensed skin WST by using the newly-developed regression equation between monthly T_w and T_s (Eq. (1)). The latter is the monthly skin WST averaged from the ASTER Surface Kinetic Temperature daily 90 m grid product (AST_08) in the present study.

$$\frac{T_w}{\overline{T_w}} = a*\frac{T_s}{\overline{T_s}} + b \tag{1}$$

where, $\overline{T_w}$and $\overline{T_s}$ are regionally averaged annual bulk WST and skin WST, e.g., the average annual values in a watershed, which are easier to access than the daily or monthly values at a point; a and b are coefficients that need to be calibrated before T_w estimation.

3.2. Calculation of the integrated degradation coefficients

The integrated degradation coefficient (k, in d^{-1}) in a river-section is often calibrated with the equation $k = 86.4\ln\left(\frac{C_0}{C_1}\right)\frac{u}{L}$ (Testa et al., 2013; Li et al., 2015) where u is the averaged hydrological streamflow velocity in a river-section (in $m\,s^{-1}$) and L is the length of the river section (in km). Additionally, the adjustment of k can be achieved by $k = 1.047^{T_w-20}k_{20}$ (CAEP, 2003; Chen et al., 2014), where k_{20} is k at 20 °C for water and T_w stands for any water temperature. Combining the above two equations, we can derive a new Eq. (2) to estimate the real-time k at any level of water temperature.

$$k = 86.4a_{20}\left(\frac{u}{L}\right)^{b_{20}+1} 1.047^{T_w-20} \tag{2}$$

where a_{20} and b_{20} are coefficients that can be easily calibrated for 20 °C using the equation $\ln\left(\frac{C_0}{C_1}\right) = a_{20}\left(\frac{u}{L}\right)^{b_{20}}$ (Wang et al., 2006) or directly using Eq. (2) based on a few observations in a straight river-section. Therefore, real-time k for a given water temperature can be calculated easily with the satellite-retrieved water temperature (T_w) in Eq. (1).

3.3. Estimation of the water environmental capacity (WEC)

The WEC allows for a certain amount of pollutants to be discharged into water bodies to ensure the concentration of pollutants are below water quality standards (Han et al., 2010; Chen et al., 2014). The calculated integrated degradation coefficient k in Section 3.2 and the water quality standard (C_s, in $mg\,l^{-1}$) for a river-section were used to calculate WEC based on Zhao et al. (2018).

$$W = (Q_0 + q)C_s - Q_0C_0e^{\frac{-kx_1}{86.4u}} \tag{3}$$

where W is the water environmental capacity, in $g\,s^{-1}$; k is the integrated degradation coefficient; q refers to the pollutant water discharge, in $m^3\,s^{-1}$; Q_0 is the river discharge through the upstream cross-sections in the studied river-section, in $m^3\,s^{-1}$; C_0 is the concentration of a certain pollutant at the upstream cross-section, in $mg\,l^{-1}$; and x_1 is the distance from a sewage outlet or water use canal source to the upstream cross-section, in km.

Water quality standard (C_s) for the studied river-section can be calculated considering the requirements of water supply. In general, the water usage requirement on pollutant concentration depends on regional land use, vegetation cover and the socio-economic development status in the adjacent terrestrial areas. The former two can be mapped via satellite images (e.g., Landsat TM 30 m grid products), and the latter is available in regional statistics records (SBS and NBS-SOS, 2007, 2008, 2009). C_s was assigned the minimum value of requirements of all water usage on a pollutant (nutrient). For additional details, please refer to Zhao et al. (2018).

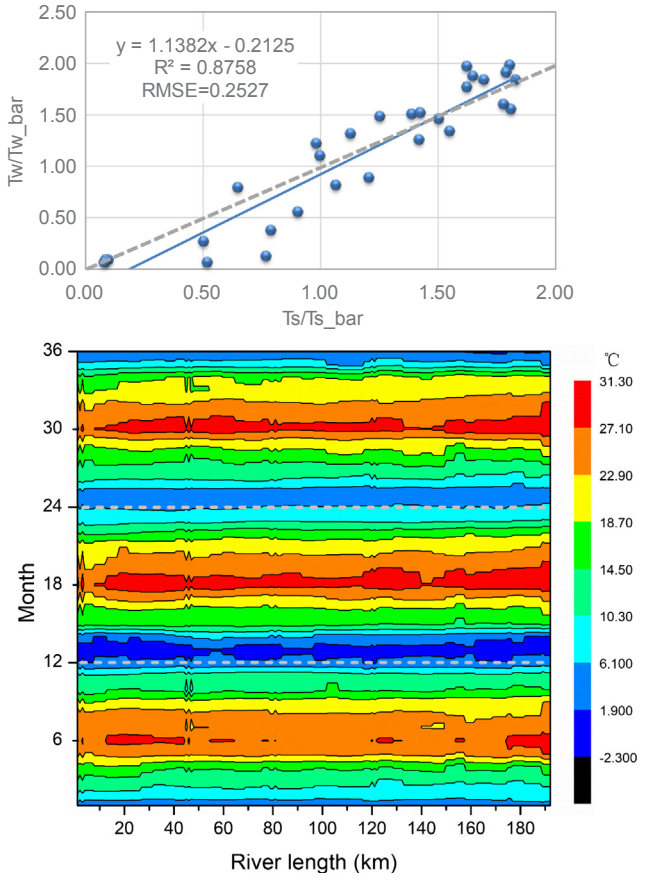

Fig. 3. Retrieval of water temperature T_w (in °C) in the river section of LJC-XY. Upper: Retrieval formula from ASTER T_s to observed T_w with dotted line being the 1:1 line and _bar representing the average; Lower: Pixel T_w retrieved from ASTER products (*Ts*, in K) along the river section. There are 36 months in the three years of 2007 through 2009. Grey dash line indicates the beginning of a subsequent year.

4. Results and Discussion

4.1. Retrieval of water temperature with satellite LST products

Daily remotely sensed skin WST (T_s) from the ASTER Surface Kinetic Temperature 90 m grid product (AST_08) in the Wei River Basin from 2007 to 2009 were initially averaged into monthly T_s (Fig. 2). Based on these data, the monthly T_s values in the Wei River were extracted.

The monthly ASTER surface temperature data at station LJC on the Wei River were then correlated with the limited historical observations of water temperature at station LJC from 2007 to 2009, and subsequently used to determine the empirical formula between the surface temperature and the water temperature based on Eq. (1), as shown in Eq. (4) and Fig. 3 (upper). With this equation, the water temperature sequence in the river section LJC-XY was generated (Fig. 3 (lower)) which can be used to calculate k in Eq. (2). Water temperature covering 36 months (2007–2009) at every pixel along the river section was retrieved. Over time, water temperature varied periodically with seasons, being high from the latter part of spring to summer (orange- and red-colored areas in Fig. 3 (lower), more than 20 °C) and low during winter (blue colors indicated areas, less than 10 °C). Spatially, it varies slowly from upstream (LJC) to downstream (XY) with almost similarly colored areas despite some small fluctuations (Fig. 3 (lower)). All these water temperature values can be used for further calculation of the degradation coefficient k with Eq. (2).

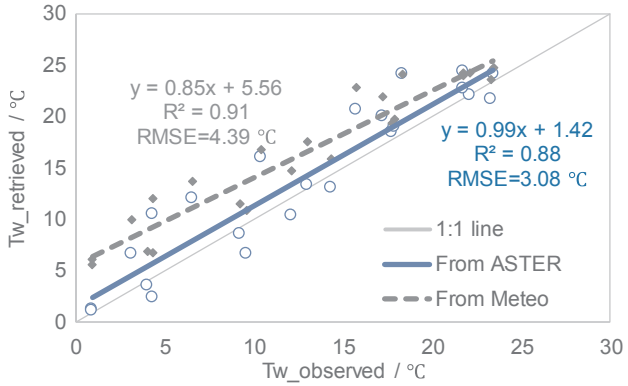

Fig. 4. Comparison of T_w observed and those retrieved from meteorological stations (T_a) and ASTER products (*Ts*).

$$T_w = \bar{T}_w\left(1.14\frac{T_s}{\bar{T}_s} - 0.21\right) \quad \text{with} \quad T_s > 273.15\,(R^2 = 0.88) \tag{4}$$

To evaluate uncertainties in water temperature assessments, an alternative data source – air temperature data (T_a) from meteorological station no. 57016 located near station LJC were analyzed together with the limited ground-based T_w measurements from Jan. 2007 to Dec. 2009 at station LJC. Using Eq. (1), a second formula to retrieve water temperature with meteorological air temperature was fitted as per Eq. (5).

$$T_w = \begin{cases} \bar{T}_w\left(0.63\frac{T_a}{\bar{T}_a} + 0.37\right) & \text{with} \quad T_a \geq 0\,(R^2 = 0.97) \\ \bar{T}_w\left(0.62\frac{T_a}{\bar{T}_a} + 0.51\right) & \text{with} \quad T_a < 0\,(R^2 = 0.91) \end{cases} \tag{5}$$

To analyze the uncertainties of the derived T_w values between different data sources, Eq. (4) was used to calculate the T_w near the hydrological station LJC based on the ASTER surface-temperature (T_s). The results were plotted in Fig. 4 to compare with T_w data derived from the meteorological air temperature (T_a) data by using Eq. (5).

T_w values generated from meteorological air-temperature data (grey diamond in Fig. 4) were greater than the T_w observations at station LJC (RMSE = 4.39 °C with R^2 = 0.91), whereas T_w values derived from the ASTER surface-temperature (blue circle in Fig. 4) were distributed evenly along the 1:1 line (RMSE = 3.08 °C with R^2 = 0.88). The reason may be that the sparse distribution of meteorological stations caused discordance in the geographical position and produced bias from T_w observations at station LJC. In contrast, the geographical position of remotely sensed T_s products concurred with that of ground T_w observations and produced a series of reasonable T_w results. Also, thermal inertia of air is very different from that of water causing bias in the T_w generated from T_a which is affected by meteorology more intensively than the water bodies.

4.2. Calculation of the integrated degradation coefficients

To calibrate a_{20} and b_{20} in Eq. (2), observations from a field trial in 2006 were used. The trial was conducted in a straight river-section of 10.35 km between stations LJC and XY (Liu et al., 2007). Based on the selected observations at 20 °C and using Eq. (2), parameters of a_{20} and b_{20} were calibrated as 1.14 and −0.11 for COD with a RMSE (root mean square error) of 1.03 d^{-1}, 1.21 and −0.03 for NH_3-N with a RMSE of 0.47 d^{-1}. Based on these parameters, two real-time k equations were obtained:

$$k = 98.35\left(\frac{u}{L}\right)^{0.89} 1.047^{T_w-20}\cdot(\text{RMSE} = 1.03\cdot d^{-1},\ R^2 = 0.99 \text{ for COD}) \tag{6}$$

and

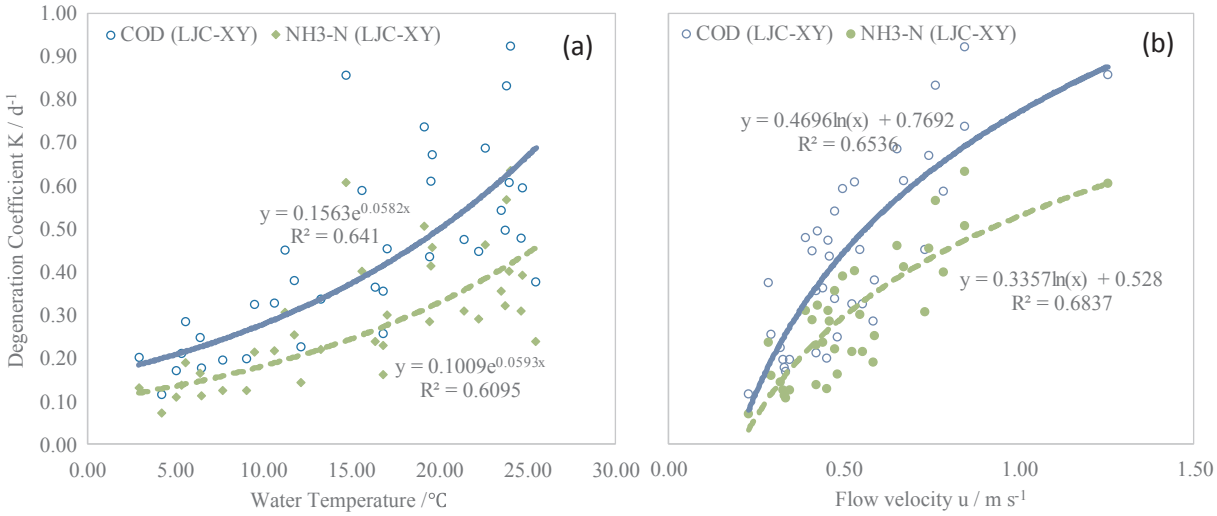

Fig. 5. The relationship between degradation coefficients (k for COD and NH_3-N) and water temperature (a), streamflow velocity (b) in the waters of LJC-XY. Partly revised from Zhao et al. (2018).

$$k = 104.37\left(\frac{u}{L}\right)^{0.97} 1.047^{T_w-20}\cdot(\mathrm{RMSE} = 0.47\cdot d^{-1},\ R^2 = 0.99\ \text{for}\ NH_3\text{–N}) \quad (7)$$

Real-time k changes with water temperature over different seasons and is also influenced by variations in hydrological streamflow velocity (Fig. 5). The above real-time k equations (Eqs. (6) and (7) subsequently were used to estimate k in the WEC of the Wei River in the following sections of this paper.

In both Eqs. (6) and (7), k can be impacted by hydrological streamflow velocity (u), river length (L) and water temperature (T_w); but the impact magnitudes of these three factors are unknown. Selection of the principal factor(s) impacting the k value is of great importance for the operation of water projects. Therefore, relationships between degradation coefficients and river length (k-L), water temperature (k-T_w) and streamflow velocity (k-u) were studied (Figs. 3 and 4).

Water temperature, streamflow velocities and river lengths in decreasing pollutant concentrations, were assumed to be important sources of uncertainties in k estimations (Liu et al., 2007; Wang et al., 2012). Thus, the river-section between LJC and XY was studied to demonstrate the influences of water temperature and streamflow velocity on k estimations based on relationships of k-T_w and k-u. Analysis of all k-related variables showed that water temperature and streamflow velocity do have the closest relationship with k (Fig. 5). But accumulation of errors in estimating T_w (Eq. (4) from the remotely sensed ASTER Surface Kinetic Temperature resulted in uncertainties in k estimates (Eqs. (6) and (7) and subsequently lowered the correlation coefficients of k with water temperature and streamflow velocity ($R^2 < 0.70$ in Fig. 5). In general for both COD and NH_3-N in the section between LJC and XY, k increased with water temperature in an exponential form. The value of k for COD was higher than that for NH_3-N based on the same hydrological streamflow velocity regime, with the correlation coefficient (R) of the former being slightly higher than that of the latter. However, the relationship between k and streamflow velocity exhibited a logarithmic form, i.e., k increased with streamflow velocity logarithmically. Specifically, k increased exponentially with water temperature and logarithmically with streamflow velocity, as indicated in the research of Zhao et al. (2018). Likewise, results from Chen et al. (2014) showed that k for both COD and NH_3-N increased with increasing water temperature. Similar to water temperature, k for COD was higher than that for NH_3-N at the same streamflow velocity.

In addition to water temperature and streamflow velocity, river length was also studied to assess its impact on k, using different lengths in a straight river section between LJC and XY. Generally, the k values for both COD and NH_3-N decreased with river length. To explore the minimum river length required for k to maintain nearly constant values for the two parameters, variations of ks and concentrations of the two parameters along with river length were plotted (Fig. 6). It shows that k decreased abruptly in the initial 1/3 of the flow path, while the decreasing trend slowed in the final 2/3 of the study section (~4–10 km). Accordingly, the concentration of the two parameters decreased rapidly with the reduction of k and reached relatively stable values after flowing more than 0.5 km. In other words, a river length of 4 km is required to attain a stable degradation coefficient which allows the pollutants (as measured by COD and NH_3-N) to sufficiently degenerate. As such the minimum river length of 4 km is required to maintain a steady k value in WEC assessments.

Overall, k for COD was higher than that for NH_3-N. In the present study, in July (2007–2009), k for COD was estimated as 0.38–0.83 d^{-1} and 0.70–1.27 d^{-1} upstream and downstream from station XY, respectively, and k for NH_3-N was estimated as 0.24–0.57 d^{-1} and 0.47–0.91 d^{-1} upstream and downstream from station XY, respectively. Liu et al. (2007) studied the degradation coefficients for both COD and NH_3-N near station XY in July 2006 and showed that the optimized k for COD was 1.03 d^{-1} and for NH_3-N was 0.67 d^{-1}, which are similar to

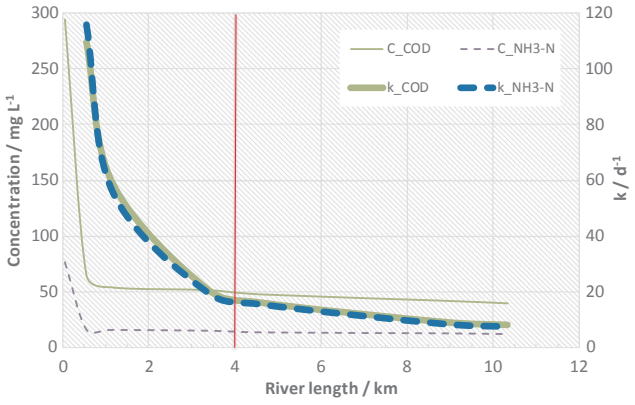

Fig. 6. The decrease of the degradation coefficients (k_{COD} and $k_{NH3\text{-}N}$, bold line) and concentrations of COD and NH_3-N (C_COD and C_NH3-N, thin line) with river length in the LJC–XY section of the Wei River. The vertical red line indicates the minimum river length of 4 km. (For interpretation of the references to colour in this figure legend, the reader is referred to the web version of this article.)

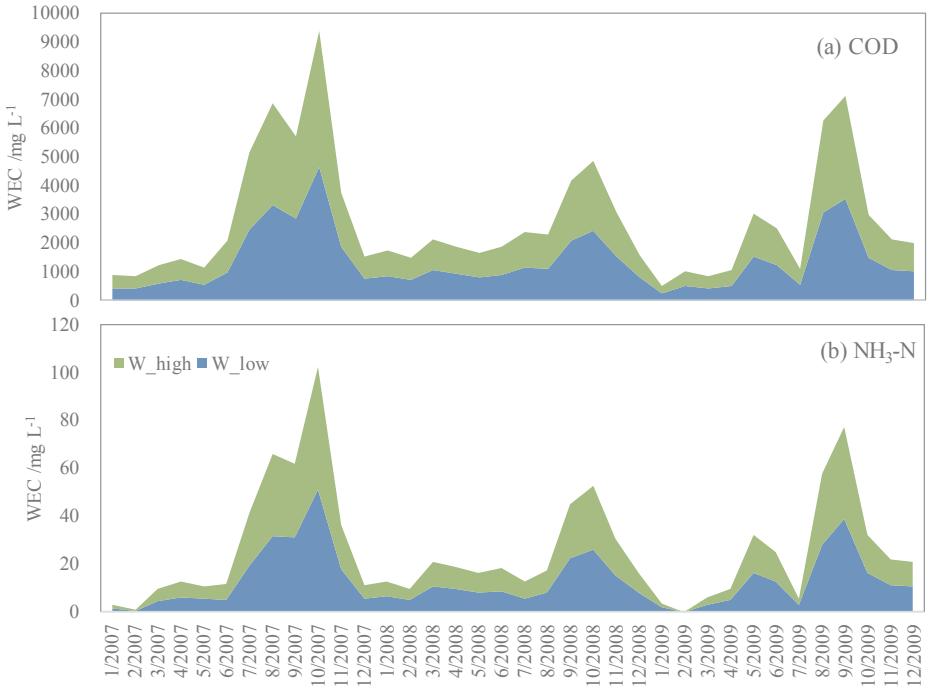

Fig. 7. Temporal variations in water environment capacity (WEC) between 2007 and 2009: the green background represents the highest WEC, while the blue represents the lowest WEC. Partly revised from Zhao et al. (2018). (For interpretation of the references to colour in this figure legend, the reader is referred to the web version of this article.)

results from the present study. Few differences exist because the variation of water temperature and streamflow velocity. Water temperature near station XY in July 2006 was 26.03 °C with a streamflow velocity of 0.46 m s^{-1} (Liu et al., 2007), while water temperature in July 2007 was 22.11 °C with a streamflow velocity of 0.97 m s^{-1}, which led to a higher *k* for COD (1.27 d^{-1}) and the second highest *k* for NH_3-N (0.91 d^{-1}). An increase in streamflow velocity in July 2007 greater than two times that in July 2006 contributed significantly to the increase in *k*s, both for COD and NH_3-N. Su (2006) studied the degeneration process of COD near station XY using water-quality data from 1992 to 2001, and found that the highest *k* for COD was 1.43 d^{-1}, close to the highest value of 1.36 d^{-1} in Aug. 2007 in our study.

4.3. Estimation of the water environmental capacity (WEC)

Both the WECs for COD and NH_3-N were estimated in the Wei River (Fig. 7). Their temporal variations concurred highly with the hydrological attributes (streamflow velocity and runoff) of the river, as well as with water temperature. The highest and lowest WECs were similar in their variations in relation to seasons. Generally, in the wet season with high streamflow velocity and water temperature (June to Oct. every year), both of them showed steep increases in WEC values. In the dry season (Nov. to May following year) the WEC values remained low with little fluctuation.

To evaluate our results, two models of Zhou et al. (1999) and Dang et al. (2009) were then adopted to study uncertainties in WEC estimation. Three rivers were selected: one in China, the Huai River, and two in Australia, the Ovens and the Gwydir Rivers (Hadwen et al., 2010). Due to the scarce data availability the WECs for only COD in the Huai River were calculated and compared, and those for only NH_3-N in the two Australian rivers were compared (Fig. 8). Like that in the Zhao et al. (2018) study, monthly river discharge datasets greater than zero in the Huai River were selected from 1998 to 2003. The WEC estimation results were then compared between the Zhou et al. (1999), Dang et al. (2009) and our models. To further test the performance of our model, we selected two rivers in Australia, the Ovens and the Gwydir Rivers, using NH_3-N concentrations to compare the three models for their performance in calculating WEC based on 12 concurrent samplings in December 2006 (Hadwen et al., 2010).

The results of our model in the Huai River, China (Fig. 8a) were between those of Zhou et al. (1999) and Dang et al. (2009) but closer to the latter model. Likewise, the WEC values based on our model in the two Australian rivers (Fig. 8b) were between those of the Zhou et al. (1999) and Dang et al. (2009) models; however, the majority of the WEC values derived from the Dang et al. (2009) model was below zero, which deviates from standard practice. This illustrates the feasibility of our model which is practical and more robust than the Dang et al. (2009) model. This also demonstrates our model's potential application in regions with insufficient ground observations. In brief, the three comparisons in the three rivers revealed that our model is practical in assessing water environment capacities and shows good potential for application to rivers with insufficient ground observations.

5. Conclusion

Comprehensive water quality data required to run water environmental capacity (WEC) models have limited their wide application in areas with limited ground observations. A new framework to estimate the WEC was presented. In this framework, water temperature was determined by using ASTER skin WST mapped from satellite images. The degradation coefficient was calculated with few water quality observations. The application of the framework in the Wei River suggest that the real-time *k* for COD is higher than that for NH_3-N, which varied with water temperature over different seasons and was also influenced by variations in streamflow velocity. The *k* value increased exponentially with increasing water temperature but logarithmically with increasing streamflow velocity. The minimum river length that assures a steady *k* value must be met before calculations can proceed. Modeling water temperatures calculated from remotely sensed land surface temperature and from meteorologically observed air temperature are promising. The accuracy of the former attribute is higher than that of the latter. The values of the former attribute were distributed evenly along the 1:1 line and had higher concurrence with ground-observed values, whereas the values of the latter attribute were much higher than that of the former, deviating from the ground observed water temperature values. This is attributed to the sparse distribution and coarse spatial resolution of the meteorological stations. Comparison with previous research and models which require comprehensive data

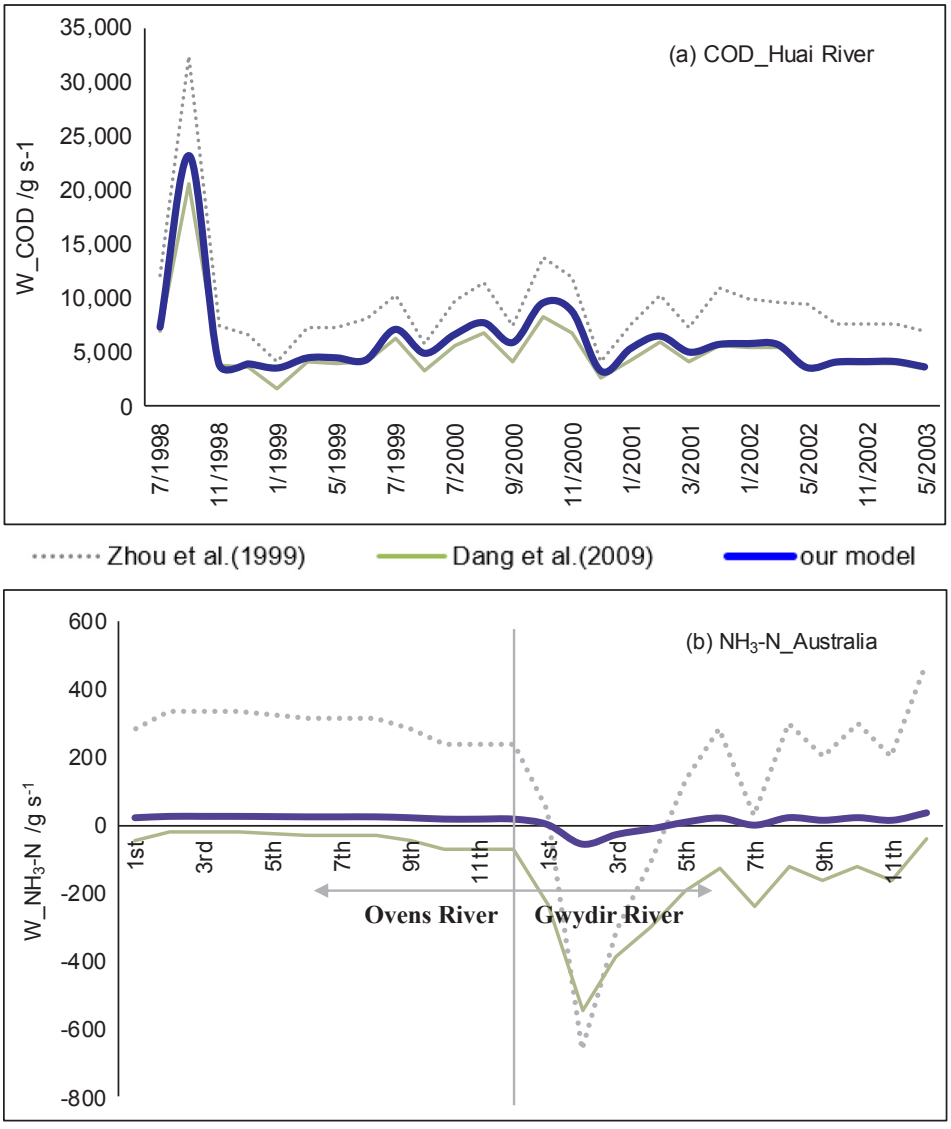

Fig. 8. Comparison of our model with those of Zhou et al. (1999) and Dang et al. (2009) in Chinese (a) and Australian rivers (b). Partly revised from Zhao et al. (2018).

reveals the practicability and effectiveness of our model, which shows promise for application to rivers with insufficient ground observations.

Acknowledgments

We acknowledge the reviewers and editors for their valuable advice on improving the quality of this paper. We thank the China Scholar Council (CSC) and our colleagues from Dalian Ocean University, Jinan and Dongying Survey Bureau of Hydrology, Institute of Geographical Science and Natural Resources Research (CAS) and Beijing Normal University for their support in funding the research and collaboration during field investigations.

This research was jointly supported by the National Key Project for R&D (Grant Numbers 2016YFC0402403 & 2016YFC0402409), the National Natural Science Foundation Program of China (Grant Number 41471340), and the Program for Key Science and Technology Innovation Team in Shaanxi province (Grant Number 2014KCT-27), China.

References

Alcântara, E.H., Stech, J.L., Lorenzzetti, J.A., Bonnet, M.P., Casamitjana, X., Assireu, A.T., de Moraes Novo, E.M.L., 2010. Remote sensing of water surface temperature and heat flux over a tropical hydroelectric reservoir. Remote Sens. Environ. 114 (11), 2651–2665.

Alcazar, J., Palau, A., Vega-Garcia, C., 2008. A neural net model for environmental flow estimation at the Ebro River Basin. Spain. J. Hydrol. 349 (1–2), 44–55.

Antonellini, M., Dentinho, T., Khattabi, A., Masson, E., Mollema, P.N., Silva, V., Silveira, P., 2014. An integrated methodology to assess future water resources under land use and climate change: an application to the Tahadart drainage basin (Morocco). Environ. Earth Sci. 71 (4), 1839–1853.

Bachmann, R.W., Hoyer, M.V., Fernandez, C., Canfield, D.E., 2003. An alternative to proposed phosphorus TMDLs for the management of Lake Okeechobee. Lake Reservoir Manage. 19, 251–264.

Brown, L.C., Barnwell, T.O., 1987. The enhanced stream water quality models QUAL2E and QUAL2E-UNCAS. New York: Documentation and User Manual, pp. 41–55.

Chen, D.J., Lu, J., Jin, S.Q., Shen, Y.N., 2007. Study on estimation and allocation of river water environmental capacity. J. Soil Water Conserv. 3, 123–127.

Chen, Q., Wang, Q., Li, Z., Li, R., 2014. Uncertainty analyses on the calculation of water environmental capacity by an innovative holistic method and its application to the Dongjiang River. J. Environ. Sci. China 26 (9), 1783–1790.

Chinese Academy for Environmental Planning (CAEP), 2003. Guidance for determination of national Water Environmental Capacity. Beijing, pp. 1–77.

Cooter, W., Rineer, J., Bergenroth, B., 2010. A nationally consistent NHDPlus framework for identifying interstate waters: implications for integrated assessments and inter-jurisdictional TMDLs. Environ. Manage. 46, 510–524.

Cuadra, M., Björklund, J., 2007. Assessment of economic and ecological carrying capacity of agricultural crops in Nicaragua. Ecol. Indic. 7, 133–149.

Dang, Z.L., Wu, B., Feng, M.Q., Hu, F., 2009. Forecast research on water environmental capacity for the water source area in Shaanxi of Middle Line of Transferring water

from south to north. J. Northwest Univ. (Nat. Sci. Ed.) 39 (4), 660–666.
Duan, S.B., Li, Z.L., Wang, N., Wu, H., Tang, B.H., 2012. Evaluation of six land-surface diurnal temperature cycle models using clear-sky in situ and satellite data. Remote Sens. Environ. 124, 15–25.
Duan, S.B., Li, Z.L., Tang, B.H., Wu, H., Tang, R.L., 2014. Generation of a time-consistent land surface temperature product from MODIS data. Remote Sens. Environ. 140, 339–349.
Environmental Protection Administration of China (EPAC), 2002. In: Environmental Quality Standards for Surface Water. GB 3838-2002. China Environmental Science Press, Beijing, pp. 1–8.
Feng, P.L., Shi, C.W., Zhang, G.L., 2004. Analysis of "2003" Weihe River flood and its disaster mitigation measures. J. China Inst. Water Resour. Hydropower Res. 2 (1), 44–60.
Gassman, P.W., Reyes, M.R., Green, C.H., Green, C.H., Arnold, J.G., 2007. The soil and water assessment tool: historical development, application, and future research directions. Am. Soc. Agric. Biol. Eng. 50 (4), 1211–1250.
Gomes, P.I., Wai, O.W., 2014. Sampling at mesoscale physical habitats to explain headwater stream water quality variations: Its comparison to equal-spaced sampling under seasonal and rainfall aided flushing states. J. Hydrol. 519, 3615–3633.
Gong, L., Jin, C.L., 2009. Fuzzy comprehensive evaluation for carrying capacity of regional water resources. Water Resour Manage. 23 (12), 2505–2513.
Guo, X., Wang, L., Wang, X., Liu, H., 2013. Occurrence and environmental risk assessment of PAEs in Weihe River near Xi'an City, China. Water Sci. Technol. 67 (5), 948–958.
Hadwen, W.L., Fellows, C.S., et al., 2010. Longitudinal trends in river functioning: patterns of nutrient and carbon processing in three Australian rivers. River Res. Appl. 26, 1129–1152.
Han, M., Mu, J., Sun, F., Cheng, L., Hao, Z., 2010. Estimation of water environment capacity: example as four basin in Shandong province, China. Proc. Environ. Sci. 2, 1919–1926.
Huang, S., Chang, J., Huang, Q., Chen, Y., 2014. Spatio-temporal changes and frequency analysis of drought in the Wei River Basin, China. Water Resour. Manage. 28 (10), 3095–3110.
Hughes, D.A., Desai, A.Y., Birkhead, A.L., Louw, D., 2014. A new approach to rapid, desktop-level, environmental flow assessments for rivers in South Africa. Hydrol. Sci. J. J. Des. Sci. Hydrol. 59 (3–4), 673–687.
Imteaz, M.A., Asaeda, T., 2000. Artificial mixing of lake water by bubble plume and effects of bubbling operations on algal bloom. Water Res. 34 (6), 1919–1929.
Joniak, T., Kuczynska-Kippen, N., 2010. The chemistry of water and bottom sediments in relation to zooplankton biocenosis in small agricultural ponds. Oceanol. Hydrobiol. Stud. 39 (2), 85–96.
Keller, A.A., Cavallaro, L., 2008. Assessing the US clean water Act 303(d) listing process for determining impairment of a water body. J. Environ. Manage. 86 (4), 699–711.
Kim, S.M., Brannan, K.M., Zeckoski, R.W., Benham, B.L., 2014. Development of total maximum daily loads for bacteria impaired watershed using the comprehensive hydrology and water quality simulation model. J. Environ. Sci. Heal. A 49, 1077–1089.
Leuning, R., Zhang, Y.Q., Rajaud, A., Cleugh, H., Tu, K., 2008. A simple surface conductance model to estimate regional evaporation using MODIS leaf area index and the Penman-Monteith equation. Water Resour. Res. 44 (10), 1–17.
Levashova, E.A., et al., 2004. Natural and human-induced variationsin water and sediment runoff in the Danube River mouth. Water Resour./Vodnye Resursy 31, 235–246.
Li, J.K., Li, H.E., Du, J., Chen, H., Shen, B., 2014. Simulation studies on the effects of integrated management measures for reducing point source and non-point source pollution in the Weihe River basin. Fresenius Environ. Bull. 23 (8a), 1920–1933.
Li, J.X., Liao, W.G., 2002. The effect of water flow on the biodegradation of organic pollutant. Res. Environ. Sci. 3, 45–48.
Li, Y.X., Qiu, R.Z., Yang, Z.F., Li, C.H., Yu, J.S., 2010. Parameter determination to calculate water environmental capacity in Zhangweinan Canal Sub-basin in China. J. Environ. Sci. 22 (6), 904–907.
Li, Z.L., Tang, B.H., Wu, H., Ren, H., Yan, G., Wan, Z., Sobrino, J.A., et al., 2013. Satellite-derived land surface temperature: Current status and perspectives. Remote Sens. Environ. 131, 14–37.
Li, H., Zhang, Y., Chiew, F.H., Xu, S., 2009. Predicting runoff in ungauged catchments by using Xinanjiang model with MODIS leaf area index. J. Hydrol. 370 (1), 155–162.
Li, K., Zhang, L., Li, Y., Zhang, L., Wang, X., 2015. A three-dimensional water quality model to evaluate the environmental capacity of nitrogen and phosphorus in Jiaozhou Bay, China. Mar. Poll. Bull. 91 (1), 306–316.
Li, R., Zou, Z., 2015. Water environmental capacity analysis of taihu lake and parameter estimation based on the integration of the inverse method and Bayesian modeling. Int. J. Environ. Res. Public Health 12 (10), 12212–12224.
Liu, R.Z., Borthwick, A.G., 2011. Measurement and assessment of carrying capacity of the environment in Ningbo, China. J. Environ. Manage. 92 (8), 2047–2053.
Liu, J., Ma, Y.G., Wang, B.Q., Zhao, C.Y., 2007. Degeneration characteristics of organic pollutant in the Xianyang Section of the Weihe River. Yellow River 29 (4), 30–40.
Liu, C.M., Zhao, C.S., Xia, J., Sun, C.L., Wang, R., Liu, T., 2011. An instream ecological flow method for data-scarce regulated rivers. J. Hydrol. 398, 17–25.
McVicar, T.R., Bierwirth, P.N., 2001. Rapidly assessing the 1997 drought in Papua New Guinea using composite AVHRR imagery. Int. J. Remote Sens. 22 (11), 2109–2128.
McVicar, T.R., Jupp, D.L., 2002. Using covariates to spatially interpolate moisture availability in the Murray-Darling Basin: a novel use of remotely sensed data. Remote Sens. Environ. 79 (2), 199–212.
Nesme, T., Toublant, M., Mollier, A., et al., 2012. Assessing phosphorus management among organic farming systems: a farm input, output and budget analysis in southwestern France. Nutr. Cycl. Agroecosyst. 92 (2), 225–236.
Pandey, V.P., Babel, M.S., Shrestha, S., Kazama, F., 2011. A framework to assess adaptive capacity of the water resources system in Nepalese river basins. Ecol. Indic. 11, 480–488.
Park, K., Jung, H.S., Ahn, S.M., 2005. Three-dimensional hydrodynamic eutrophication model (HEM-3D): application to Kwang-Yang Bay, Korea. Mar. Environ. Res. 60 (2), 171e193.
Payandeh, A., Zaker, N.H., Niksokhan, M.H., 2015. Numerical assessment of nutrient assimilative capacity of Khur-e-Musa in the Persian Gulf. Environ. Monit. Assess, 187.
Rui, Y., Shen, D., Khalid, S., Yang, Z., Wang, J., 2015. GIS-based emergency response system for sudden water pollution accidents. Phys. Chem. Earth 79–82, 115–121.
Shaanxi Bureau of Statistics (SBS) and NBS Survey Office in Shaanxi (NBS-SOS), 2007. Shaanxi Statistical Yearbook. China Statistics Press.
Shaanxi Bureau of Statistics (SBS) and NBS Survey Office in Shaanxi (NBS-SOS), 2008. Shaanxi Statistical Yearbook. China Statistics Press.
Shaanxi Bureau of Statistics (SBS) and NBS Survey Office in Shaanxi (NBS-SOS), 2009. Shaanxi Statistical Yearbook. China Statistics Press.
Smirnov, A., Holben, B.N., Eck, T.F., Dubovik, O., Slutsker, I., 2000. Cloud-screening and quality control algorithms for the AERONET database. Remote Sens. Environ. 73, 337–349.
Song, J.X., Xu, Z.X., Liu, C.M., Li, H.E., 2007. Ecological and environmental instream flow requirements for the Wei River – the largest tributary of the Yellow River. Hydrol. Process. 21 (8), 1066–1073.
Su, Y., 2006. Management System for Aquatic Environment in the River-section near Xianyang Station. Master Dissertation of Xi'an University of Technology, Xi'an.
Tang, R.L., Li, Z.L., Tang, B., 2010. An application of the T s–VI triangle method with enhanced edges determination for evapotranspiration estimation from MODIS data in arid and semi-arid regions: implementation and validation. Remote Sens. Environ. 114 (3), 540–551.
Tang, R.L., Li, Z.L., Jia, Y., Li, C., Sun, X., Kustas, W.P., Anderson, M.C., 2011. An intercomparison of three remote sensing-based energy balance models using large aperture scintillometer measurements over a wheat–corn production region. Remote Sens. Environ. 115 (12), 3187–3202.
Tang, R.L., Li, Z.L., 2017. An end-member-based two-source approach for estimating land surface evapotranspiration from remote sensing data. IEEE Trans. Geosci. Remote Sens. 55 (10), 5818–5832.
Teggi, S., Despini, F., 2014. Estimation of subpixel MODIS water temperature near coastlines using the SWTI algorithm. Remote Sens. Environ. 142, 122–130.
Testa, J.M.Q., Brady, D.C., Toro, D.M.D., Boynton, W.R., Cornwell, J.C., Kemp, W.M., 2013. Sediment flux modeling: simulating nitrogen, phosphorus, and silica cycles. Estuar. Coast. Shelf Sci. 131, 245–263.
Thiemann, S., Schiller, H., 2003. Determination of the bulk temperature from NOAA/AVHRR satellite data in a midlatitude lake. Int. J. Appl. Earth Obs. Geoinf. 4 (4), 339–349.
Torgersen, C.E., Faux, R.N., McIntosh, B.A., Poage, N.J., Norton, D.J., 2001. Airborne thermal remote sensing for water temperature assessment in rivers and streams. Remote Sens. Environ. 76 (3), 386–398.
Wan, W., et al., 2017. A comprehensive data set of lake surface water temperature over the Tibetan Plateau derived from MODIS LST products 2001–2015. Sci. Data 4, 170095.
Wan, Z.W., Yuan, Y.L., Qiao, F.L., 2001. 2-order turbulence closure plankton ecosystem dynamics model and its application. J. Hydrodynam. Ser. B 3, 17–23.
Wang, S., Xu, L., Yang, F., Wang, H., 2014. Assessment of water ecological carrying capacity under the two policies in Tieling City on the basis of the integrated system dynamics model. Sci. Total Environ. 472, 1070–1081.
Wang, L., Zhang, H.O., Xie, J.C., Luo, J.G., Yan, L., 2012. Research on dynamic characteristics of river pollution degradation coefficient between Longmen and Sanmenxia on the Yellow River. J. Xi'an Univ. Technol. 28 (3), 294–298.
Wang, Y.L., Zhou, Z.F., Wang, L.J., et al., 2006. Test on degradation coefficient of ammonia-nitrogen in Yellow River adjacent to Lanzhou. J. Lanzhou Univ. Technol. 32 (5), 72–74.
Wang, H., Zhou, Y., Tang, Y., Wu, M., Deng, Y., 2015. Fluctuation of the water environmental carrying capacity in a huge river-connected lake. Int. J. Environ. Res. Public Health 12 (4), 3564–3578.
Wright, R.M., Mcdonell, A.J., 1979. Instream deoxygenation rate prediction. Proc ASCE J. Environ. Div 105 (4), 323–333.
Wu, W., Xu, Z.X., Yin, X.W., Yu, S.Y., 2014a. Fish community structure and the effect of environmental factors in the Wei River basin. Acta Sci. Circumstantiae 34 (5), 1298–1308.
Wu, W., Xu, Z., Yin, X., Zuo, D., 2014b. Assessment of ecosystem health based on fish assemblages in the Wei River basin, China. Environ. Monit. Assess. 186 (6), 3701–3716.
Yang, J., Lei, K., Khu, S., Meng, W., Qiao, F., 2015. Assessment of water environmental carrying capacity for sustainable development using a coupled system dynamics approach applied to the Tieling of the Liao River Basin, China. Environ. Earth Sci. 73 (9), 5173–5183.
Yang, Z.F., Sun, T., Zhao, R., 2014. Environmental flow assessments in estuaries related to preference of phytoplankton. Hydrol. Earth Syst. Sci. 18 (5), 1785–1791.
Yoon, T., Rhodes, C., Shah, F.A., 2015. Upstream water resource management to address downstream pollution concerns: a policy framework with application to the Nakdong River basin in South Korea. Water Resour. Res. 51 (2), 787–805.
Yu, X., Geng, Y., Heck, P., Xue, B., 2015. A Review of China's rural water management. Sustainability 7 (5), 5773–5792.
Zhang, G., et al., 2014a. Estimating surface temperature changes of lakes in the Tibetan Plateau using MODIS LST data. J. Geophys. Res.: Atmos. 119, 8552–8567.
Zhang, Y., Chiew, F.H., Zhang, L., Li, H., 2009. Use of remotely sensed actual evapotranspiration to improve rainfall-runoff modeling in Southeast Australia. J. Hydrometeorol. 10 (4), 969–980.
Zhang, Y., Leuning, R., Hutley, L.B., Beringer, J., McHugh, I., Walker, J.P., 2010. Using

long-term water balances to parameterize surface conductances and calculate evaporation at 0.05 spatial resolution. Water Resour. Res. 46 (5), 1–14.
Zhang, Z., Lu, W.X., Zhao, Y., Song, W.B., 2014b. Development tendency analysis and evaluation of the water ecological carrying capacity in the Siping area of Jilin Province in China based on system dynamics and analytic hierarchy process. Ecol. Model. 275, 9–21.
Zhang, Y., Wang, X.Y., Zhang, Z.M., Shen, B.G., 2012. Multi-level waste load allocation system for Xi'an-Xianyang Section, Weihe River. Proc. Environ. Sci. 13, 943–953.
Zhao, C.S., Yang, S.T., Liu, J.G., et al., 2018. Linking fish tolerance to water quality criteria for the assessment of environmental flows: a practical method for streamflow regulation and pollution control. Water Res. 141, 96–108.
Zhou, X.D., Guo, J.L., Cheng, W., Song, C., Cao, G., 1999. The comparison of the environmental capacity calculation methods. J. Xi'an Univ. Technol. 15 (3), 1–6.
Zuo, D., Xu, Z., Wu, W., Zhao, J., Zhao, F., 2014. Identification of streamflow response to climate change and human activities in the Wei River Basin, China. Water Resour. Manage. 28 (3), 833–851.